Biochemical Society Transactions (2020) **48** 1683–1696
https://doi.org/10.1042/BST20200164

PORTLAND PRESS

Review Article

Plant transporters involved in combating boron toxicity: beyond 3D structures

Maria Hrmova[1,2], Matthew Gilliham[1,3] and Stephen D. Tyerman[1,3]

[1]School of Agriculture, Food and Wine, University of Adelaide, Waite Campus, South Australia 5064, Australia; [2]School of Life Science, Huaiyin Normal University, 223300 Huai'an, China; [3]Australian Research Council Centre of Excellence in Plant Energy Biology, University of Adelaide, Waite Campus, South Australia 5064, Australia

Correspondence: Maria Hrmova (maria.hrmova@adelaide.edu.au)

Membrane transporters control the movement and distribution of solutes, including the disposal or compartmentation of toxic substances that accumulate in plants under adverse environmental conditions. In this minireview, in the light of the approaching 100th anniversary of unveiling the significance of boron to plants (K. Warington, 1923; *Ann. Bot.* **37**, 629) we discuss the current state of the knowledge on boron transport systems that plants utilise to combat boron toxicity. These transport proteins include: (i) nodulin-26-like intrinsic protein-types of aquaporins, and (ii) anionic efflux (borate) solute carriers. We describe the recent progress made on the structure–function relationships of these transport proteins and point out that this progress is integral to quantitative considerations of the transporter's roles in tissue boron homeostasis. Newly acquired knowledge at the molecular level has informed on the transport mechanics and conformational states of boron transport systems that can explain their impact on cell biology and whole plant physiology. We expect that this information will form the basis for engineering transporters with optimised features to alleviate boron toxicity tolerance in plants exposed to suboptimal soil conditions for sustained food production.

Boron — significance, toxicity, tolerance, regulation and sensing

Boron and plants

In the soil, boron (B) is a naturally occurring trace metalloid that is indispensable for plant development and growth [1]. Depending on pH, B occurs in the form of the boric acid (BA) $B(OH)_3$ and tetrahydroxy borate anions $[B(OH)_4]^-$. BA, as a weak Lewis acid with pK_a of 9.24 can readily interreact in cells with a variety of biological molecules that are typically in excess of the cellular BA concentrations [2]. As BA is uncharged at neutral or acidic pH, it can readily enter cells via passive diffusion (Figure 1a), although at a lower rate than other small amphipathic (with polar and apolar parts) molecules [3,4]. In soils, B is thought to be a highly mobile element but is often one of the more deficient among trace elements.

In plants, B is involved in a variety of cellular, physiological and metabolic processes including transport of sugars, photosynthesis, cell wall synthesis, maintenance of the plasma membrane integrity and function, catalysis as a cofactor, and the metabolism of carbohydrates, nucleic acids, and nitrogen-containing, indoleacetic and phenolic compounds [4]. It has been accepted that one of the major functions of B is in the structure of primary plant cell walls, forming the rhamnogalacturonan-II-boron 1 : 2 diol ester complexes (Figure 1b) that are vital for the assembly of pectin networks that underlie cell wall strength and flexibility [5,6].

Received: 22 May 2020
Revised: 15 July 2020
Accepted: 17 July 2020

Version of Record published:
11 August 2020

Biochemical Society Transactions (2020) 48 1683–1696
https://doi.org/10.1042/BST20200164

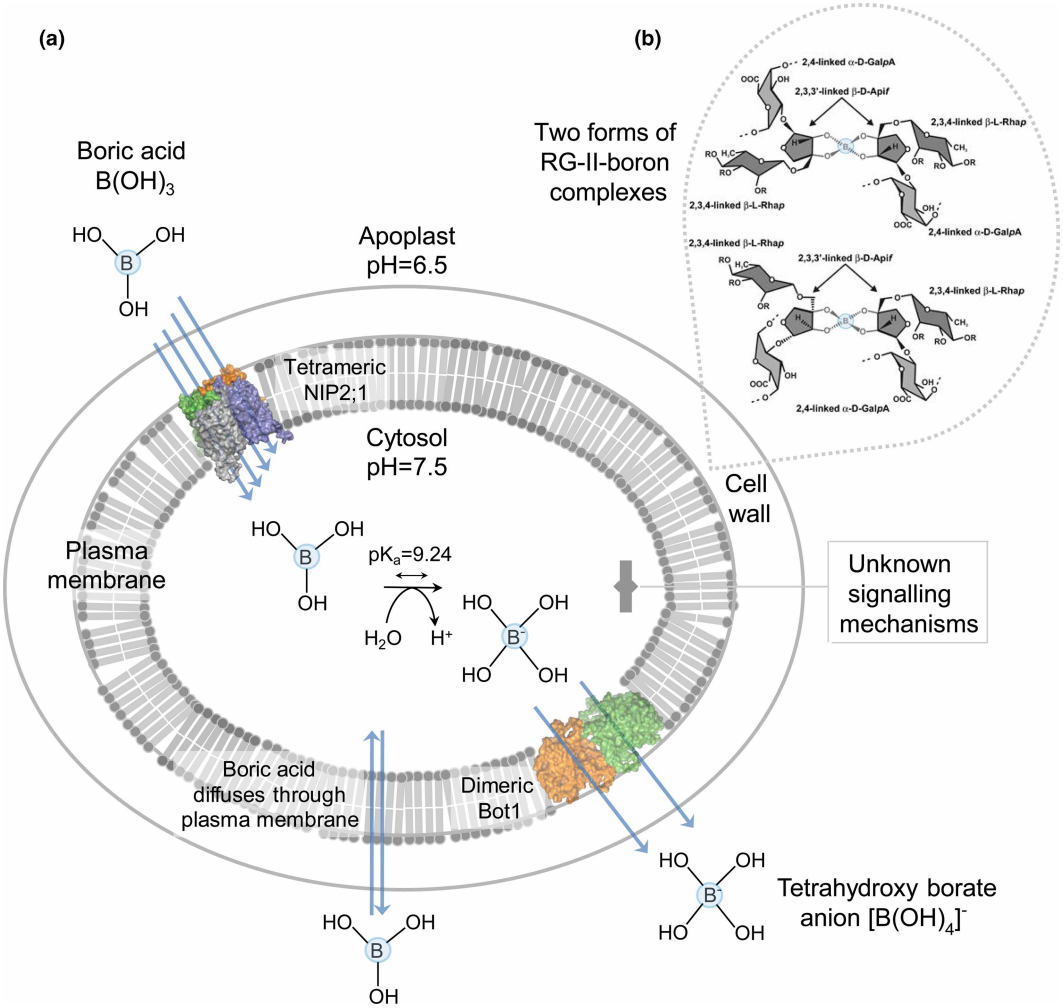

Figure 1. Mechanism of soil B toxicity tolerance that regulates plant tissue B homeostasis.

(**a**) In plants, at least two types of membrane transport proteins are known to lower the intracellular B concentration during excessive soil B. Signalling mechanisms that sense high soil B are unknown. The multifunctional barley NIP2;1 aquaporin (*cf.* Figure 2) [15] permeates BA [$B(OH)_3$] in the neutral form, while the barley Bot1 [17] and *Arabidopsis* BOR1 [58] efflux transporters (*cf.* Figure 3) permeate tetrahydroxy borate anions $[B(OH)_4]^-$. BA also enters cells through the plasma membrane without the assistance of transporters (double arrow). Quaternary homotetrameric NIP2;1 and homodimeric BOR1 in the plasma membrane are illustrated in surface representations, with protomers coloured in green, orange, deep blue and grey (NIP2;1) or green and orange (BOR1). Multiple blue arrows drawn through monomers illustrate influx of $B(OH)_3$ via NIP2;1, or efflux of $[B(OH)_4]^-$ through BOR1. BA with pK_a of 9.24 occurs in the apoplast (pH = 6.5) in a neutral form and is converted to $[B(OH)_4]^-$ in the cytosol at pH = 7.5. The pH values were determined by non-invasive imaging [90]. (**b**) One of the key biological function of B is in cross-linking two rhamnogalacturonan-II (RG-II) monomers through the branched pentose apiosyl sugar residues, forming two types of borate 1 : 2 diol ester complexes. These reversible RG-II-B pectin complexes are required for biogenesis and structure of plant cell walls [5,6]. B atoms in each RG-II molecule are circled in blue.

B toxicity in plants caused by high soil B

Under adequate B supply, its uptake from soil to plants through roots is largely driven by a passive process (Figure 1a). However, high soil and irrigation water B contents lead to B toxicity that is endemic across the world and was identified in a range of plant species. Geographically, B toxicity is known in the Middle East (Iraq, Pakistan, Afghanistan), South (India) and Eastern (China) Asia, South (Peru, Chile, Colombia, Argentina) and North (the US) America, North Africa (Algeria, Libya, Morocco), Mediterranean Europe

(Spain) and South and Western Australia [7,8]. B toxicity is the problem particularly in dry areas leading to revenue losses, e.g. in some areas of Australia the yield penalties for wheat and barley could be up to 8–11% [9,10]; these losses rival other stresses like salinity [11].

How plants respond to high soil B and tolerance mechanisms: current models

In all plant species, the primary mechanism of B toxicity tolerance is associated with a limited entry of B, in the form of BA in the roots and the disposal of BA excess through leaf hydathodes [7]. Typical symptoms of B toxicity include leaf burn, necrosis and discolorations, delayed plant growth and development including root growth retardation that together lead to diminished fruit and seed yields [4,7,12]. In most plant species, after B is absorbed by roots, it is loaded into the xylem and translocated to shoots via the transpiration stream and accumulated in older leaves without being re-distributed; for this reason, there is a direct relationship between the B content in leaves and the severity of toxicity symptoms [3]. Notably, toxicity symptoms are more severe in shoots than roots due to the down-regulation of genes encoding root- and shoot-specific aquaporins that lead to the reduction in cell-to-cell water movement and the water flux to shoots [13]. If the toxic effects of B persist, the suppression of nitrogen and sugar metabolism develop [4,14] owing to the high reactivity of B towards poly-hydroxy groups in molecules with a *cis*-configuration. These cytotoxic effects cause metabolic disturbance and oxidative stress, where ribose is the primary target molecule that typically fulfils a key role in energy metabolism, photosynthesis and gene expression [4].

In cereals like barley, two types of passive transporters (Figure 1a), without a need for energy input, have been implicated in B toxicity tolerance: (i) the multifunctional NIP2;1 (nodulin-26-like intrinsic protein) aquaporin that permeates water and metalloids, such as BA in a neutral form [15], and (ii) the Bot1 anion efflux (borate) transporter that conducts BA and other anions in negatively charged forms [16–18].

Significant attention was paid to the function of NIP-type aquaporins [15,19] and borate efflux transporters (Bot1 and BOR-like) *in planta* [7,12,20–23]. Under the excess of soil B, the regulatory mechanisms drove up the expression of the barley *Bot1* or *Arabidopsis BOR4* genes to increase mRNA transcript levels [12,20]; in contrast, the expression of NIPs was down-regulated via mRNA degradation [15,19]. Under high soil B the shoot growth was decreased, and the shoot B levels increased in the *Arabidopsis* T-DNA insertion mutants of *BOR4* that was detected in root meristems and endodermis. Increased *BOR4* mRNA levels in roots indicated that *BOR4* was B-inducible and BOR4 was functional [20]. But, under the adequate B supply, the expression of the xylem *BOR1* B-exporter gene (paralog of *BOR4*) was down-regulated in *Arabidopsis* due to the selective BOR1 degradation via B-dependent translational suppression mechanisms [21]; three putative tyrosine and acidic di-leucine motifs involved in this regulation were identified [22]. It was shown that under limited B, *Arabidopsis* NIP5;1 and BOR1 localised to the soil- and stele-sides of plasma membrane regions in root cells, respectively [23].

The primary sensing mechanisms of exogenous B concentrations in plants, presumably at the apoplastic or cytoplasmic levels have not been defined. However, it was suggested in other plant systems that multiple sensing mechanisms could detect ions at the plasma membrane levels by means of receptor-like kinases [24] or sense stress-induced cell wall damage [25].

Structural mechanisms of transporters involved in B toxicity tolerance

The barley multifunctional NIP aquaporins permeate and co-permeate water, metalloids and a variety of other solutes in neutral forms

The 'aquaporin' term was coined by Agre et al. [26] to describe the major intrinsic proteins that facilitate the rapid and selective movement of water in the direction of the osmotic gradient. The aquaporin family consist of five sub-families that have specialised in their function during evolution, comprising of nodulin-26-like intrinsic proteins (NIPs), plasma membrane intrinsic proteins (PIPs), tonoplast intrinsic proteins (TIPs), small basic intrinsic proteins (SIPs) and X-intrinsic proteins (XIPs). Each has structural features (Figure 2) that underlie their physicochemical properties and transport function [27]. From these five subgroups, primarily NIPs [28] and Solanaceae XIPs [29,30] — both weakly water-permeable — transport BA and other metalloids such as silicic, arsenious and germanic acids; these aquaporins are also known as 'metalloido-porins' [31]. It was proposed that the NIP archetypical aquaporins have evolved from bacterial ancestors [32].

Biochemical Society Transactions (2020) **48** 1683–1696
https://doi.org/10.1042/BST20200164

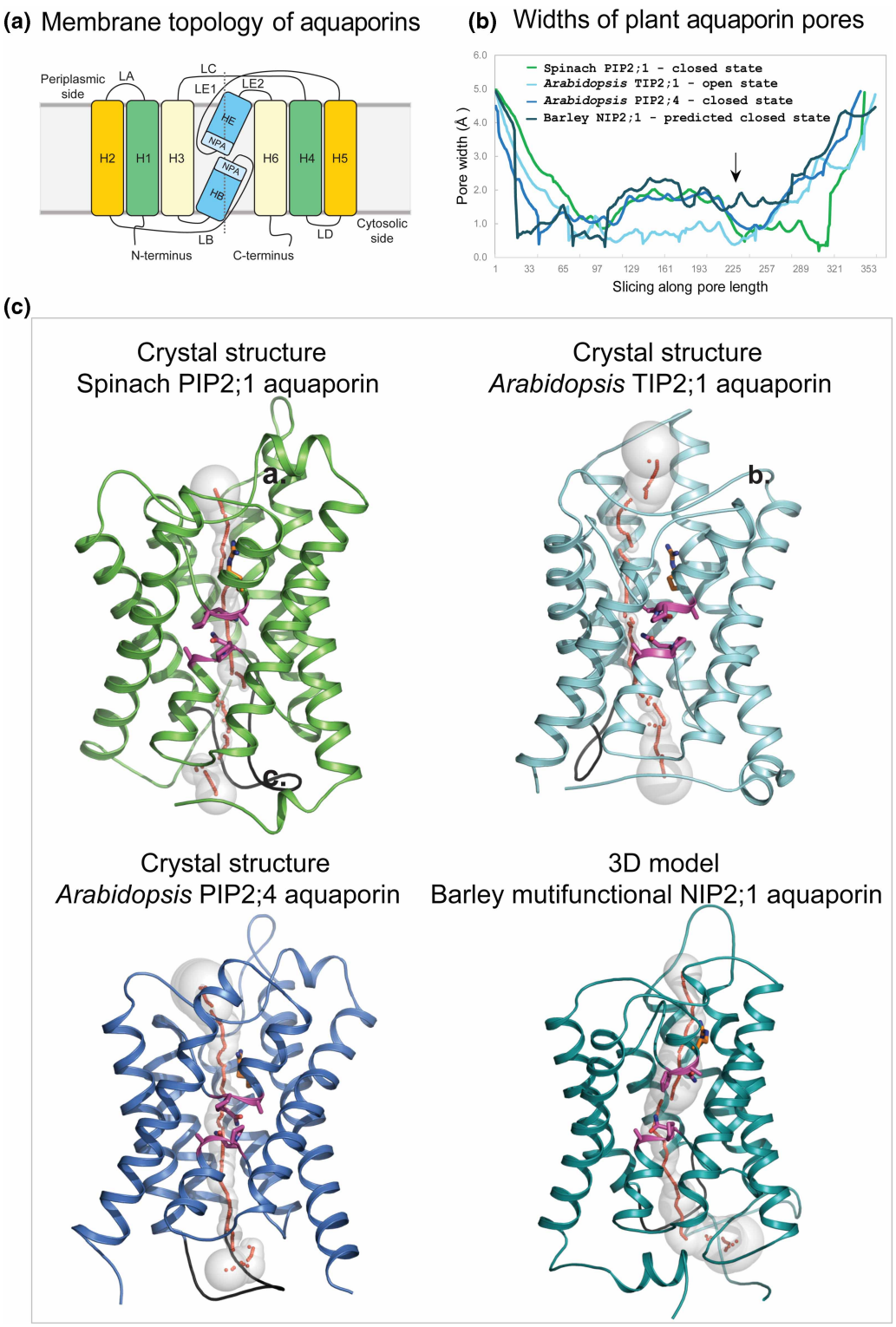

Figure 2. Molecular structures of plant aquaporins involved in water, metalloid, ion and other solute transport.

Part 1 of 2

(**a**) Membrane topology diagram of aquaporins. Each aquaporin molecule consists of six H1–H6 transmembrane α-helices (orange, green, pale yellow boxes) and two re-entrant HB and HE α-helices (marine). Transmembrane α-helices are inter-connected via five LA–LE loops. Two Asn-Pro-Ala (NPA) motifs HE (flanked by LE1 and LE2 loops) and HB (flanked by LB

Figure 2. Molecular structures of plant aquaporins involved in water, metalloid, ion and other solute transport. Part 2 of 2

loop) (aquamarine) are separated by ∼4–5 Å. The dotted line separates bipartite structural repeats of hour-glass folded aquaporins. (**b**) Profiles of pore width parameters of aquaporins (in Å) calculated by Hole [91] and conformational states (closed or open) of spinach PIP2;1 (PDB 1z98; green), and *Arabidopsis* TIP2;1 (PDB 5i32; cyan) and PIP2;4 (PDB 6qim; deep blue) aquaporins. The 3D model of barley NIP2;1 (teal) was built by trRosetta [38] as described in the text. Barley NIP2;1 has a wider pore (arrow) along its entire length, compared with those of predominantly water-permeable aquaporins. (**c**) Cartoon representations of monomeric aquaporins (colouring as described above) enclose pores with morphologies shown by sequences of grey spheres (pore radii are equal to sphere diameters) and red dots. Two conserved NPA motifs (magenta sticks) (*cf.* panel (**a**)) and neighbouring Arg222 (one of the selectivity filter residues, orange sticks) line pores in central regions. LD loops (black) show similar dispositions in all aquaporins and are assumed to be essential for pore closure at cytosolic sides of proteins. In barley NIP2;1 the last 20 residues were omitted for clarity.

The architecture of an aquaporin monomer — a structural sub-unit of a functional aquaporin tetramer — consists of six tilted membrane-spanning α-helices (H1–H3 and H4–H6) and two short re-entrant α-helices (HB and HE) running in two repeats with five interconnecting loops (LA–LE) forming a right-handed α-helical bundle (Figure 2). A solute-permeating pore traverses each monomer that can be of various morphology and thickness. In the barley multifunctional NIP2;1 aquaporin, the pore is, in particular, wide along its entire length compared with PIPs and TIPs (Figure 2b,c), which predominantly permeate water and are important for diminishing water potential gradients and rapid cell volume fluctuations, e.g. those that underlie stomatal dynamics [33]. This unusual width of the pore in barley NIP2;1 and most likely other NIP isoforms allows for the transport of various uncharged solutes such as glycerol, lactic acid, BA and other metalloids, although this list is incomplete as a whole spectrum of other solutes has not yet been examined. Because of selectivity, NIPs have been described as the functional equivalents of aquaglyceroporins (a subset of aquaporins permeating a wide range of small uncharged solutes) found in all domains of life [34]. The broad selectivity of NIPs and aquaglyceroporins is underpinned by the selectivity filter signatures and the pore structural features [18,27]. It is noteworthy that the cytosolic loops D (LD) (Figure 2a,c-coloured in black) show similar spatial dispositions in various aquaporins, e.g. in spinach PIP2;1 (Protein Data Bank-PDB 1z98) [35] and *Arabidopsis* PIP2;4 (PDB 6qim) [36] and TIP2;1 (PDB 5i32) [37], and barley NIP2;1 — for this assessment we built the 3D model of NIP2;1 by trRosetta [38] using spatial restraints and alignments of more than 49 000 sequences. The finding of similar spatial dispositions of D loops amongst various aquaporins is intriguing. It was shown in spinach PIP2;1 that this loop, together with His193 and dephosphorylation of conserved Ser residues triggered pore closure [35]. This suggests that the structural dynamics of PIPs, TIPs and NIPs could be similar.

It is noteworthy that α-helices that are significantly tilted in aquaporin structures follow a pseudo-two-fold axis that runs at an approximate 90° angle to a membrane normal, thus sub-dividing an hour-glass aquaporin into bipartite segments. In native environments, individual solute-permeating monomers form a quaternary functional tetramer. Here, four protomers come together along the four-fold rotational axis to create a tightly fitted tetrameric trapezoid architecture that leads to the formation of an additional central 'fifth' pore, which in some aquaporins could provide an extra permeation route. In this context, through molecular dynamics (MD) simulations, the geometric and kinetic aspects of so-called electro-pores or ionic conductivity pores were described in human aquaporin 4 in their entire lengths [39,40]. This work showed that aquaporin 4 mediated the sustained conductivity of anionic (Cl^-) and cationic (Na^+ and Ca^{2+}) species through the solute-permeating and central electro-pores due to the presence of predominantly hydrophobic residues lining each pore. However, a cautionary note is that electric fields, used in these works, could induce mechanical disruptions to aquaporin pores and simulated fluxes — this involves high electric field strengths that are much larger than those formed in aquaporins under the physiological conditions.

Furthermore, the importance of solute-permeating and central pores is relevant to human aquaporins 1 and 6, and *Arabidopsis* PIPs, which when expressed in *Xenopus* oocytes, induced non-selective ion conductance that may be indicative of water and ion transport [41–44] — this could take place through the central pore [45]. This additional pore may function in BA-permeating NIP aquaporins that could conduct small ionic species together with BA. But, how the transport of ionic species precisely happens in aquaporins at the structural levels remains to be established.

Biochemical Society Transactions (2020) **48** 1683–1696
https://doi.org/10.1042/BST20200164

It is important to mention the significance of the extended NH_2- and COOH-terminal sequence regions specific to the barley NIP2;1 aquaporin (Figure 2c), as these extensions may regulate transport function and the formation of complexes with other non-transporting protein partners at the membrane level. These regions contain post-translational modification sites (e.g. phosphorylation, acetylation, methylation, deamidation, ubiquitination, N- and O-linked glycosylation sites) and signatures [46,47] for binding of structurally ordered proteins (e.g. kinases), or highly flexible partially disordered (or completely disordered) proteins that occupy larger volumes [48]. Such interactions are vital for aquaporins as they could modulate membrane properties that in turn influence trafficking and signalling. Binding of these non-transporting proteins could cause steric and lateral pressure that induces an irregular curvature in membranes; this could even lead to the formation of membrane sub-compartments [48].

The N- and C-terminal end-localised post-translational phosphorylation sites in *Arabidopsis* NIPs are subject to modifications by calcium-dependent protein kinases (consensus sequence: hydrophobic-X-basic-X-X-Ser/Thr) or mitogen-activated protein kinases (Pro-X-Ser/Thr-Pro) [49]. More specifically, the B-permeable subgroup II *Arabidopsis* NIP7;1 contains the Arg-Pro-Cys-Pro-Ser-Pro-Val-Ser-Pro-Ser motif (consensus underlined) located on the C-terminal loop [49]. Similarly, C-terminal phosphorylation sites in the B-permeable subgroup I *Arabidopsis* NIP4;1 and NIP4;2 are known; these sites are modified by pollen-specific calcium-dependent protein kinases that adjust their water permeability [50]. Notably, terminal Ser in the *Arabidopsis* NIP7;1 motif and C-terminal Ser residues in *Arabidopsis* NIP4;1 and NIP4;2 confine to the comparable positions than Ser274 (that triggered pore closure) in spinach PIP2;1 [35]. This once again points out that the dynamics of PIP, TIP and NIP aquaporins could be similar. Conversely, the triple repeat ThrProGly motif that in the B-permeable subgroup II *Arabidopsis* NIP5;1 is present at the N-terminal end, was found to be modified by mitogen-activated protein kinases [49,51]. This phosphorylation motif, which is necessary for the efficient uptake of B by root cells, was localised on the soil-side plasma membrane region (as opposed to the stele-side) of the outermost root cell layers and is maintained by the clathrin-mediated endocytosis [51]. As for the mechanisms that direct the localisation of membrane proteins in a polar manner, the process is complex and includes high or low phosphorylation states of proteins [51].

We have already mentioned that extended NH_2- and COOH-terminal regions of aquaporins often participate in the formation of multi-membrane complexes that originate through the binding of non-transporting partners. These proteins do not interact directly with transporters but could change the stability and excitability (or voltage dependency) of transporters, as it was shown in the human acid-sensing ion channel using combined patch-clamp electrophysiology and fluorescence resonance energy transfer [52]. As for aquaporins, interactomics and protein binding networks in PIP2;1 from *Arabidopsis* root cells revealed that these proteins could operate as platforms for the recruitment of a wide range of transport activities [53]. This study provided a novel insight into the regulation of cellular trafficking how lipid signalling affected water-permeable PIPs, and how protein kinases (e.g. receptor-like kinases and Feronia) differentially modulated the PIP activity through separate regulatory mechanisms. Furthermore, the function of 14-3-3 proteins in the recruitment of kinases that phosphorylate *Arabidopsis* PIP2;1 was described and how these modifications affected circadian regulation of hydraulic conductivity in leaves [54]. Similar studies are required for BA-permeable NIP2;1 to explain the significance of unusually protracted NH_2- and COOH-terminal regions (Figure 2c).

The barley anion efflux transporter Bot1 conducts borate (with high affinity) and other anions (with low affinity)

Barley Bot1 is classified amongst the solute carrier (SLC) superfamily of transporters in the Anion Exchanger family 2.A.31 [55]. This transporter conducts charged tetrahydroxyborate anions $[B(OH)_4]^-$ (Figure 1a) with a high affinity, and Cl^-, PO_4^{3-}, SO_4^{2-} and NO_3^- ions with a low affinity [17]. However, the cell does not appear to sacrifice the loss of essential anionic nutrients (and thus energy) through the efflux via the Bot1 transporter in favour of tissue B homeostasis. It is fundamental to answer how the structure of Bot1 is crucial to selectivity that allows the cell to exclude toxic borate anions whilst retaining anionic nutrients.

In this group of transporters, the structurally related pro- and eukaryotic SLC4, SLC23 and SLC26 transporter families have been studied for nearly a decade. The first crystal structure of one of these transporters, the homodimeric *Escherichia* UraA uracil transporter (PDB 3qe7; SLC23) [56] was elucidated in an inward-facing conformation and was used as a paradigm structure for these families. Within the next 5 years, four other crystal structures of SLC homodimers followed and included the human anion exchanger — band 3 in

Biochemical Society Transactions (2020) **48** 1683–1696
https://doi.org/10.1042/BST20200164

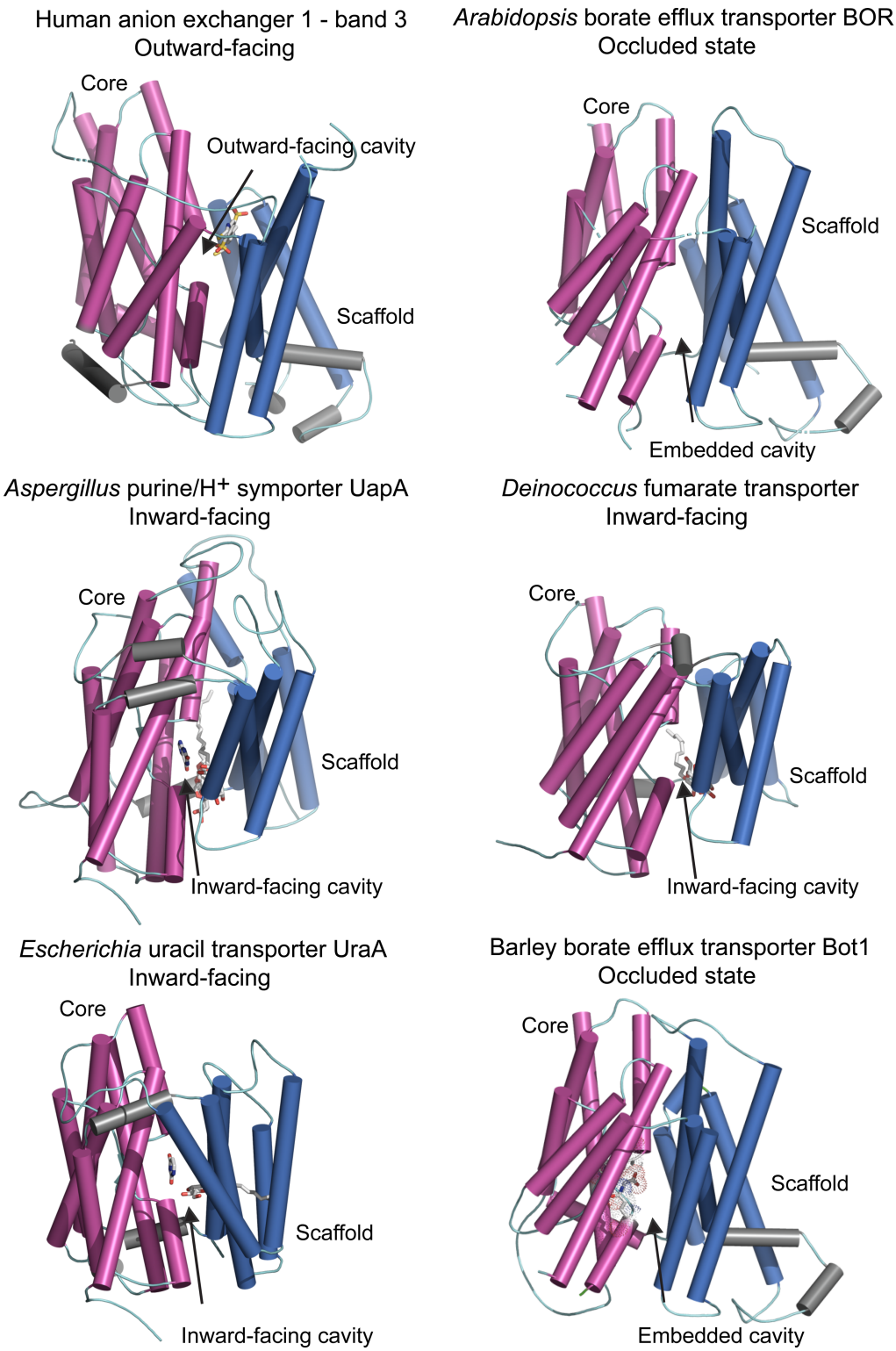

Figure 3. Molecular structures of the elevator-type transporters that permeate a variety of solutes. Part 1 of 2

Cartoon representations of monomeric efflux transporters with membrane cylindrical α-helices indicating conformational states. Cartoons of human anion exchanger — band 3 (PDB 4yzf), *Arabidopsis* BOR1 borate efflux transporter (PDB 5l25), *Aspergillus* UapA purine/H^+ symporter (PDB 5i6c), *Deinococcus* fumarate transporter (PDB 5da0) and *Escherichia* UraA uracil transporter (PDB 3qe7) illustrate dispositions of core (magenta) relative to those of scaffold (gate) (deep blue) domains, and additional

Biochemical Society Transactions (2020) **48** 1683–1696
https://doi.org/10.1042/BST20200164

Figure 3. Molecular structures of the elevator-type transporters that permeate a variety of solutes. Part 2 of 2

α-helices (grey). Arrows indicate dispositions of outward- and inward-facing or embedded cavities containing bound solutes (grey sticks). UapA, fumarate and UraA structures contain dodecyl-β-D-maltoside surfactant, *n*-nonyl-β-D-maltoside surfactant, and n-nonyl-β-D-glucoside surfactant and the pyrimidine ring of uracil, respectively (grey sticks). 3D model (based on the 5l25 template) of the barley efflux transporter Bot1 is included for comparison, where the longest intervening loops adjoining cylindrical α-helices were omitted for clarity. CPK sticks with dots, illustrating Van der Waals radii indicate the positions of highly conserved Ala96, Asp317, Asn361 and Gln366 residues that are likely to be involved in the permeation of $[B(OH)_4]^-$ by barley Bot1.

an outward-facing conformation (PDB 4yzf; SLC4) [57] the *Arabidopsis* BOR1 borate efflux transporter in an occluded conformation (PDB 5l25; SLC4) [58], the *Deinococcus* fumarate transporter (PDB 5da0; SLC26) [59] and the *Aspergillus* UapA purine/H^+ symporter (PDB 5i6c; SLC23) [60]; the last three structures were reported in an inward-facing state (Figure 3). Recently, the cryo-electron microscopy structure of the human NBCe1 sodium-coupled acid–base transporter, in an outward-facing conformation became available (PDB 6caa; SLC4) [61]. Additionally, Figure 3 presents the 3D model of the barley efflux transporter Bot1 that was previously built using the UraA template [17,56]. This model with associated electrophysiology studies using *Xenopus* oocytes and co-translationally incorporated Bot1 in giant liposomes revealed that Bot1 mediated a Na^+-dependent polyvalent anion transport in a Nernstian manner with channel-like characteristics. The structural fold of barley Bot1 model agreed with the *Arabidopsis* BOR1 crystal structure that was elucidated some eight months later [58]. To assign the candidate residues that mediate the conductance of $[B(OH)_4]^-$ in Bot1, we present the updated 3D model based on *Arabidopsis* BOR1 [58] built as described [17]. The Bot1 structure contains in the core domain an embedded cavity, formed by short α-helices and loops carrying Ala96, Asp317, Asn361 and Gln366 residues (Figure 3) that could be involved in the $[B(OH)_4]^-$ permeation.

Although the SLC transporters are not structurally identical, they seem to operate via a similar molecular mechanism that could be accomplished in several comparable ways and is known as the 'elevator'-type. The structural basis of these mechanisms was recently reviewed with a comprehensive list of elevator-type transporters [62; *vide infra* Table 1]. Thus, we will refrain from a detailed description of the molecular mechanism of the elevator-type transport and refer the reader to this article, albeit in brief, we will mention its key features.

The elevator-transport mechanisms are based on the presence of two distinct core and scaffold (or gate) domains in transporters (highlighted in magenta and deep blue, respectively, in Figure 3) that slide across each other in the membrane as independent rigid bodies and pull the permeated solute inside a cavity. One important aspect of SLCs are opening and closing events of the scaffold domain that opens at the opposite sides of a membrane, so their gates must work in a synchronised manner; these opening and closing events may operate on millisecond time scales as defined in a kinetic model [63]. For BOR1 and Bot1 SLC4 transporters, this provides alternating access via core domains that carry borate anions across a membrane [58]. The molecular details of these motions are yet to be established, but one such hypothesis assumes that once anions are exported, they change their ionisation states and cannot be transported back. It is of note that in barley Bot1, using patch-clamp electrophysiology, we observed extended opening intervals (up to several seconds) [17; *vide infra* Figure 6]. Assuming an independent operation of each monomer in SLC4 transporters [64], the gate stayed open longer under specific voltage and ion concentrations in Bot1. This could be due to more complex motions of core and scaffold domains than simple translations leading to extended elevator events. Alternatively, Na^+ which is essential for borate anions conductance by Bot1 [17], may keep the gates open for prolonged periods. Such a mechanism could suggest a link between B toxicity and salinity, although the precise relationship between these two traits in plants is unclear [65]. These observations indicate that in defining ion permeation mechanisms, transport kinetics and current fluctuations need to be combined with structural factors. Studies of transporters are often complemented by MD simulations to gain insights into the dynamics of transporters. This dynamic is affected by oligomeric assemblies and how they perturb membrane properties in bilayers forming unique protein–lipid fingerprints [66]; those may also affect elevator movements [67].

One aspect of the structural considerations involves a homodimer assembly of SLC transporters (Figure 1a) formed *in crystallo* [56–61], similar to that of the *Arabidopsis* NRT1.1 nitrate transporter (PDB 5a2n and 4oh3) [68,69]. Here, it is important to bridge the information obtained from crystal structures with that at the cellular and physiological levels, as it was shown for NRT1.1. An elegant MD study [70] demonstrated that in NRT1.1

a dimeric switch plays a key role in eliciting cytosolic Ca^{2+} waves that are perceived by a calcineurin-B-like sensor, which in turn activates the CIPK23 kinase. Subsequent phosphorylation of NRT1.1 stabilises its monomeric state that acts as a high-affinity nitrate transporter *cum* sensor. This phosphorylation-led modulation of the activity illustrates a bistable performance of NRT1.1 that is regulated by the 'incoherent feed-forward loop' cycle involving both decoupling and coupling of the homodimer.

Progress in biotechnologies enhances definitions of transporter's mechanics

Definitions of precise molecular mechanisms and structural dynamics of transporters, comprising those involved in tissue B homeostasis, is contingent on the state-of-the-art of available technologies. Here, we report on selected membrane protein know-hows that include addressing bottlenecks and combining tasks in parallel to integrate gene expression and cloning, and protein production, scale-up, purification, and functional descriptions to better understand transporter's mechanics.

One of the progressive membrane protein production approaches includes high-yield and high-titer cellular bioproduction systems [71] in synthetic biology cell-free protein synthesis open formats [72,73] harboured in minimal cells and microfluidic devices [74]. These robust micro-reactors and micro-compartments offer novel platforms and integrate tasks in parallel, where the emphasis is on a low cost and convenience (e.g. ultra-centrifugation-free membrane protein isolation) [75], yet achieving a rapid high-throughput characterisation of membrane proteins.

Until now, the primary methods for obtaining membrane protein structures have relied on crystallisation from detergents forming micelles around hydrophobic proteins. Membrane proteins become surrounded by detergent molecules that are lipid bilayer mimetics and could initiate structural artefacts in membrane proteins. This represents a significant risk of arriving at the compromised conformational states of transporters. To counteract these artefacts, which arise from the complexity of protein–lipid interactions [76], as a start, it is imperative to avoid de-lipidation (i.e. to keep intact annular lipids that coexist with membrane proteins in native bilayers) and prepare protein crystals from high-lipid-detergent concentrations and bicelles or using lipid cubic phases (LCPs) with native lipids. One particular method of membrane protein isolation using detergent-free native cell membranes are the styrene maleic acid copolymer-lipid nanoparticles (SMALP) and their derivatives [77,78]; this approach has now been applied to several transporters [79]. It is a consensus that SMALP with LCP platforms will be the preferred methods for structural analyses of membrane transporters in the future.

To access the high-resolution and accurate structural information of transporters and to derive data of functional proteins, a combination of X-ray diffraction and micro-crystal electron diffraction [80] — using crystalline samples in native lipids and combined with *in meso in situ* serial X-ray crystallography [81] — is the preferred method. Furthermore, these analyses could be combined with cryo-electron microscopy [82] that images membrane proteins in lipid environments without crystallisation requirements.

X-ray crystallography has made and continues to make key contributions in the transporter structural field, often with anomalous scattering on improved synchrotron beamlines. This approach allows investigating the precise identity of bound ionic species to define their permeation mechanics — this was achieved with the *Streptomyces* K^+ ion channel KcsA (PDB 1k4c), where the high-quality crystallographic data allowed discussing the soft or hard knock-on transport mechanism of KcsA [83].

As for the molecular architectures of B transport systems, it is notable that the crystal structures of seemingly complex *Arabidopsis* BOR1, and related bacterial or mammalian SLC4 anion efflux transporters are available (Figure 3) [56–61]; all SLC4 proteins were expressed in microbial hosts or purified from mammalian tissues. Additionally, the crystal structures of PIP [35,36] and TIP [37] aquaporins, derived from *Pichia*-expressed proteins are accessible (Figure 2) but not those of NIPs — the reasons for this enigma could be several. One is that NIPs are structurally unique as far as they contain numerous post-translationally modifiable phosphorylation and O-linked glycosylation sites on extended N- and C-terminal regions; these are longer than those of PIPs and TIPs. These regions may be required for NIPs to fold and form diffracting crystals with interpretable electron density maps. Including these regions together with testing different fusions with or without binding partners, combined with SMALP and LCP platforms and *in situ* and microfocus beamline X-ray crystallography or cryo-electron microscopy [80–82], could lead to success. Other options include using cost-effective expression systems for high yields of folded NIPs — e.g. transient [84,85] or stable [86] plant systems allow for folding

Biochemical Society Transactions (2020) **48** 1683–1696
https://doi.org/10.1042/BST20200164

and multimeric protein assembly. With the latter systems, the yields and quality of expressed NIPs could be better than those stemming from the traditionally used microbial hosts.

One last tool that needs to be mentioned is the use of quasi-atomistic approach to modelling of proteo-liposomes [87] in the small-angle scattering (SAS) methodology [88] using X-ray or neutron radiation that provides integral characteristics of proteo-liposomes with embedded transporters. This SAS approach considers the curvature and lateral pressure in proteo-liposomes in native bilayer or non-bilayer lipids [89] and allows the shape evaluation of transporters and their dynamics in liposomal environments.

In summary, resolving the structure–function relationships of B-transport systems with such techniques using natural and synthetic biology approaches will provide avenues for understanding B toxicity stress perception and associated mechanisms. This information will guide the engineering of transporters with optimised features that will work in plants when exposed to high soil B. The key question of all is if the engineering better B-transport systems than those that already exist in B-tolerant plants will be achieved for the benefit of food security, safety and sustainability.

Perspectives

- **Importance in the field**: It is a consensus that B toxicity tolerant plants accumulate lower levels of BA and its anions than intolerant ones implying that exclusion facilitated by membrane transporters is the key route for alleviating B toxicity and mediating tissue B homeostasis. This model is important but is incomplete and calls for multidisciplinary studies of quantitative transport analyses combined with characterisations of transporters conformational states and how these states are regulated and linked to transport.

- **Summary of current thinking**: Permeation of B transport systems and the primary sensing mechanisms of B toxicity, and how these two components are integrated into plant cell physiology, will have the paramount importance in understanding the concept of mineral (in this case B) toxicity in plants and how to bioengineer optimised transporters. Because the structure underlies transport function, as a precautionary measure, we need to acquire structures of transporters lacking artefacts.

- **Future directions**: It will be important to answer: (i) How the oligomeric NIP aquaporin assemblies are formed, and how post-translational modifications and pH regulate transport dynamics; (ii) What structural determinants play roles in the recognition of B-containing and other solutes, and if they are co-transported; (iii) Could the selectivity of Bot1 anion transporters be fine-tuned by maximising the efflux of toxic B-containing solutes and minimising the efflux of essential nutrient ions, through the identification of natural variants or bioengineering of more selective Bot1 efflux transporters? (iv) Could anion efflux transporters sense B through post-translational modulation as it was suggested for the NRT1.1 transporter, as dimerisation appears to be conserved in SLC transporter families?

Competing Interests

The authors declare that there are no competing interests associated with the manuscript.

Open Access

Open access for this article was enabled by the participation of University of Adelaide in an all-inclusive *Read & Publish* pilot with Portland Press and the Biochemical Society under a transformative agreement with CAUL.

Author Contributions

M.H. prepared figures and wrote the article. M.G. and S.D.T. contributed to writing.

Acknowledgements

This work was supported by funding from the University of Adelaide (Australia) and the Huaiyin Normal University (China) to M.H., and by the Australian Research Council Centre of Excellence in Plant Energy Biology (CE1400008) to S.T.D. and M.G. The authors are grateful to Debra Mohen for providing Figure 1b. The authors thank the anonymous reviewers for their contribution to the peer review of this work.

Abbreviations

B, boron; BA, boric acid; BOR1, *Arabidopsis* borate efflux transporter 1; BOR4, *Arabidopsis* borate efflux transporter 4; Bot1, Barley borate efflux transporter 1; H, α-helix; KcsA, *Streptomyces* K^+ ion channel; L, loop; LCP, lipid cubic phase; MD, molecular dynamics; NIP, nodulin-26-like intrinsic protein; NPA, Asn-Pro-Ala; NRT1.1, *Arabidopsis* nitrate transporter 1.1; PDB, Protein Data Bank; PIP, plasma membrane intrinsic protein; RG-II, rhamnogalacturonan-II; SAS, small-angle scattering; SIP, small basic intrinsic protein; SLC, solute carrier; SMALP, styrene maleic acid copolymer-lipid particle; TIP, tonoplast intrinsic protein; UapA, *Aspergillus* purine/H^+ symporter; UraA, *Escherichia* uracil transporter; XIP, X-intrinsic protein.

References

1 Warington, K. (1923) The effect of boric acid and borax on the broad bean and certain other plants. *Ann. Bot.* **37**, 629–672 https://doi.org/10.1093/oxfordjournals.aob.a089871
2 Woods, W.G. (1996) A review of possible boron speciation relating to its essentiality. *J. Tr. Elem. Exp. Med.* **9**, 153–163 https://doi.org/10.1002/(SICI)1520-670X(1996)9:4<153::AID-JTRA3>3.0.CO;2-S
3 Reid, R. (2014) Understanding the boron transport network in plants. *Plant Soil* **385**, 1–13 https://doi.org/10.1007/s11104-014-2149-y
4 Princi, M.P., Lupini, A., Araniti, F., Longo, C., Mauceri, A., Sunseri, F. et al. (2016) Boron toxicity and tolerance in plants: recent advances and future perspectives. In *Plant Metal Interaction* (Parvaiz, A., ed.), pp. 115–147, Elsevier Inc., ISBN 9780128031582
5 O'Neill, M.A. and York, W.S. (2003) The composition and structure of plant primary cell walls. In *The Plant Cell Wall* (Rose, J.K.C., ed.), pp. 1–54, Blackwell Publishing Ltd., ISBN 1-84127-328-7
6 Caffall, K.H. and Mohnen, D. (2009) The structure, function and biosynthesis of plant cell wall pectic polysaccharides. *Carbohydr. Res.* **28**, 1879–1900 https://doi.org/10.1016/j.carres.2009.05.021
7 Pallotta, M., Schnurbusch, T., Hayes, A., Hay, A., Baumann, U., Paull, J. et al. (2014) Molecular basis of adaptation to high soil boron in wheat landraces and elite cultivars. *Nature* **514**, 88–91 https://doi.org/10.1038/nature13538
8 Yau, S.K. (2010) Boron toxicity in barley genotypes: effects of pattern and timing of boron application. *Commun. Soil Sci. Plant Anal.* **41**, 144–154 https://doi.org/10.1080/00103620903426956
9 Schnurbusch, T., Hayes, J. and Sutton, T. (2010) Boron toxicity tolerance in wheat and barley: Australian perspectives. *Breeding Sci.* **60**, 297–304 https://doi.org/10.1270/jsbbs.60.297
10 Moody, D.B., Rathjen, A.J. and Cartwright, B. (1993) Yield evaluation of a gene for boron tolerance. In *Genetic Aspects of Plant Mineral Nutrition* (Randall, P., Delhaize, E., Richards, R.A. and Munns, R., eds), pp. 363–366, Kluwer Academic Publishers, Dordrecht, The Netherlands
11 McDonald, G., Taylor, J.D., Verbyla, A. and Kuchel, H. (2013) Assessing the importance of subsoil constraints to yield of wheat and its implications for yield improvement. *Crop Pasture Sci.* **63**, 1043–1065 https://doi.org/10.1071/CP12244
12 Sutton, T., Baumann, U., Hayes, J., Collins, N.C., Shi, B.J., Schnurbusch, T. et al. (2007) Boron-toxicity tolerance in barley arising from efflux transporter amplification. *Science* **318**, 1446–1449 https://doi.org/10.1126/science.1146853
13 Macho-Rivero, M.A., Herrera-Rodríguez, M.B., Brejcha, R., Schäffner, A.R., Tanaka, N., Fujiwara, T., et al. (2018) Boron toxicity reduces water transport from root to shoot in Arabidopsis plants. Evidence for a reduced transpiration rate and expression of major PIP aquaporin genes. *Plant Cell Physiol.* **59**, 836–844 https://doi.org/10.1093/pcp/pcy026
14 Shireen, F., Nawaz, M.A., Chen, C., Zhang, Q., Zheng, Z., Sohail, H. et al. (2018) Boron: functions and approaches to enhance its availability in plants for sustainable agriculture. *Int. J. Mol. Sci.* **19**, 1856 https://doi.org/10.3390/ijms19071856
15 Schnurbusch, T., Hayes, J., Hrmova, M., Baumann, U., Ramesh, S.A., Tyerman, S.D. et al. (2010) Boron toxicity tolerance in barley through reduced expression of the multifunctional aquaporin, HvNIP2;1. *Plant Phys.* **153**, 1706–1715 https://doi.org/10.1104/pp.110.158832
16 Hayes, J.E. and Reid, R.J. (2004) Boron tolerance in barley is mediated by efflux of boron from the roots. *Plant Phys.* **136**, 3376–3382 https://doi.org/10.1104/pp.103.037028
17 Nagarajan, Y., Rongala, J., Luang, S., Sing, A., Shadiac, N., Hayes, J. et al. (2016) A barley efflux transporter operates in a Na^+-dependent manner, as revealed through a multidisciplinary platform. *Plant Cell* **28**, 202–218 https://doi.org/10.1105/tpc.15.00625
18 Hrmova, M. and Gilliham, M. (2018) Plants fighting back: to transport or not to transport, this is a structural question. *Curr. Opin. Plant Biol.* **46**, 68–76 https://doi.org/10.1016/j.pbi.2018.07.006
19 Yoshinari, A. and Takano, J. (2017) Insights into the mechanisms underlying boron homeostasis in plants. *Front. Plant Sci.* **8**, 1951 https://doi.org/10.3389/fpls.2017.01951
20 Miwa, K., Aibara, I. and Fujiwara, T. (2014) *Arabidopsis thaliana BOR4* is upregulated under high boron conditions and confers tolerance to high boron. *Soil Sci. Plant Nutr.* **60**, 349–355 https://doi.org/10.1080/00380768.2013.866524
21 Aibara, I., Hirai, T., Kasai, K., Takano, J., Onouchi, H., Naito, S. et al. (2018) Boron-dependent translational suppression of the borate exporter *BOR1* contributes to the avoidance of boron toxicity. *Plant Physiol.* **177**, 759–774 https://doi.org/10.1104/pp.18.00119
22 Wakuta, S., Mineta, K., Amano, T., Toyoda, A., Fujiwara, T., Naito, S. et al. (2015) Evolutionary divergence of plant borate exporters and critical amino acid residues for the polar localization and boron-dependent vacuolar sorting of AtBOR1. *Plant Cell Physiol.* **56**, 852–862 https://doi.org/10.1093/pcp/pcv011

23 Takano, J., Tanaka, M., Toyoda, A., Miwa, K., Kasai, K., Fuji, K. et al. (2010) Polar localization and degradation of *Arabidopsis* boron transporters through distinct trafficking pathways. *Proc. Natl. Acad. Sci. U.S.A.* **107**, 5220–5225 https://doi.org/10.1073/pnas.0910744107
24 Feng, W., Kita, D., Peaucelle, A., Cartwright, H.N., Doan, V., Duan, Q. et al. (2018) The FERONIA receptor kinase maintains cell-wall integrity during salt stress through Ca^{2+} signaling. *Curr. Biol.* **28**, 666–675 https://doi.org/10.1016/j.cub.2018.01.023
25 Nongpiur, R.C., Singla-Pareek, S.L. and Pareek, A. (2020) The quest for osmosensors in plants. *J. Exp. Bot.* **71**, 595–607 https://doi.org/10.1093/jxb/erz263
26 Agre, P., Sasaki, S. and Chrispeels, J. (1993) Aquaporins: a family of water channel proteins. *Am. J. Physiol. Ren. Physiol.* **265**, F461 https://doi.org/10.1152/ajprenal.1993.265.3.F461
27 Luang, S. and Hrmova, M. (2017) Molecular mechanisms of function of plant aquaporins. In *Signaling, Communication in Plants, From Transport to Signalling, Plant Aquaporins* (Chaumont, F. and Tyerman, S.D., eds.), pp. 1–28, Springer, Verlag, ISBN 978-3-319-49393-0
28 Diehn, T.A., Bienert, M.D., Pommerrenig, B., Liu, Z., Spitzer, C., Bernhardt, N. et al. (2019) Boron demanding tissues of *Brassica napus* express specific sets of functional Nodulin26-like Intrinsic Proteins and BOR1 transporters. *Plant J.* **100**, 68–82 https://doi.org/10.1111/tpj.14428
29 Bienert, G.P., Bienert, M.D., Jahn, T.P., Boutry, M. and Chaumont, F. (2011) Solanaceae XIPs, members of a new aquaporin subfamily, are plasma membrane channels facilitating the transport of various uncharged solutes. *Plant J.* **66**, 306–317 https://doi.org/10.1111/j.1365-313X.2011.04496.x
30 Bienert, M.D., Muries, B., Crappe, D., Chaumont, F. and Bienert, G.P. (2019) Overexpression of X intrinsic protein 1;1 in *Nicotiana tabacum* and *Arabidopsis* reduces boron allocation to shoot sink tissues. *Plant Direct* **3**, e00143 https://doi.org/10.1002/pld3.143
31 Pommerrenig, B., Diehn, T.A. and Bienert, G.P. (2015) Metalloido-porins: Essentiality of nodulin 26-like intrinsic proteins in metalloid transport. *Plant Sci.* **238**, 212–227 https://doi.org/10.1016/j.plantsci.2015.06.002
32 Pommerrenig, B., Diehn T, A., Bernhardt, N., Bienert M, D., Mitani-Ueno, N., Fuge, J. et al. (2020) Functional evolution of nodulin 26-like intrinsic proteins: from bacterial arsenic detoxification to plant nutrient transport. *New Phytol.* **225**, 1383–1396 https://doi.org/10.1111/nph.16217
33 Ding, L. and Chaumont, F. (2020) Are aquaporins expressed in stomatal complexes promising targets to enhance stomatal dynamics? *Front. Plant Sci.* **11**, article 458 https://doi.org/10.3389/fpls.2020.00458
34 Mukhopadhyay, R., Bhattacharjee, H. and Rosen, B.P. (2014) Aquaglyceroporins: generalized metalloid channels. *Biochim. Biophys. Acta* **1840**, 1583–1591 https://doi.org/10.1016/j.bbagen.2013.11.021
35 Törnroth-Horsefield, S., Wang, Y., Hedfalk, K., Johanson, U., Karlsson, M., Tajkhorshid, E. et al. (2006) Structural mechanism of plant aquaporin gating. *Nature* **439**, 688–694 https://doi.org/10.1038/nature04316
36 Wang, H., Schoebel, S., Schmitz, F., Dong, H. and Hedfalk, K. (2020) Characterization of aquaporin-driven hydrogen peroxide transport. *Biochim. Biophys. Acta Biomembr.* **1862**, 183065 https://doi.org/10.1016/j.bbamem.2019.183065
37 Kirscht, A., Kaptan, S.S., Bienert, K.P., Chaumont, F., Nissen, P., de Groot, B.L. et al. (2016) Crystal structure of an ammonia-permeable aquaporin. *PLoS Biol.* **14**, e1002411 https://doi.org/10.1371/journal.pbio.1002411
38 Yang, J., Anishchenko, I., Park, H., Peng, Z., Ovchinnikov, S. and Baker, D. (2020) Improved protein structure prediction using predicted interresidue orientations. *Proc. Natl. Acad. Sci. U.S.A.* **117**, 1496–1503 https://doi.org/10.1073/pnas.1914677117
39 Marracino, P., Bernardi, M., Liberti, M., Del Signore, F., Trapani, E., Gárate, J.-A. et al. (2018) Transprotein-electropore characterization: a molecular dynamics investigation on human AQP4. *ACS Omega* **3**, 15361–15369 https://doi.org/10.1021/acsomega.8b02230
40 Bernardi, M., Ghaani, M.R. and English, N.J. (2020) Ionic conductivity along transmembrane-electropores in human aquaporin 4: calcium effects from non-equilibrium molecular dynamics. *Mol. Phys.* **117**, 3783–3790 https://doi.org/10.1080/00268976.2019.1665725
41 Yasui, M., Hazama, A., Kwon, T.H., Nielsen, S., Guggino, W.B. and Agre, P. (1999) Rapid gating and anion permeability of an intracellular aquaporin. *Nature* **402**, 184–187 https://doi.org/10.1038/46045
42 Yool, A.J., Stamer, W.D. and Regan, J.W. (1996) Forskolin stimulation of water and cation permeability in aquaporin1 water channels. *Science* **273**, 1216–1218 https://doi.org/10.1126/science.273.5279.1216
43 Byrt, C.S., Zhao, M., Kourghi, M., Bose, J., Henderson, S.W., Qiu, J. et al. (2017) Non-selective cation channel activity of aquaporin AtPIP2;1 regulated by Ca^{2+} and pH. *Plant Cell. Environ.* **40**, 802–815 https://doi.org/10.1111/pce.12832
44 Kourghi, M., Nourmohammadi, S., Pei, J.V., Qiu, J., McGaughey, S., Tyerman, S.D. et al. (2017) Divalent cations regulate the ion conductance properties of diverse classes of aquaporins. *Int. J. Mol. Sci.* **18**, 2323 https://doi.org/10.3390/ijms18112323
45 Yu, J., Yool, A.J., Schulten, K. and Tajkhorshid, E. (2006) Mechanism of gating and ion conductivity of a possible tetrameric pore in aquaporin-1. *Structure* **14**, 1411–1423 https://doi.org/10.1016/j.str.2006.07.006
46 Wang, D. and Liu, D. (2017) *MusiteDeep: A deep-learning framework for protein post-translational modification site prediction*, In *2017 IEEE International Conference on Bioinformatics and Biomedicine (BIBM)*, Kansas City, MO, pp. 2327–2327
47 Singh, R.K., Deshmukh, R., Muthamilarasan, M., Rani, R. and Prasad, M. (2020) Versatile roles of aquaporin in physiological processes and stress tolerance in plants. *Plant Phys. Biochem.* **149**, 178–189 https://doi.org/10.1016/j.plaphy.2020.02.009
48 Fakhree, M.M., Blum, C. and Claessens, M.M.A.E. (2019) Shaping membranes with disordered proteins. *Arch. Biochem. Biophys.* **677**, 108163 https://doi.org/10.1016/j.abb.2019.108163
49 Wallace, I.S., Choi, W.G. and Roberts, D.M. (2006) The structure, function and regulation of the nodulin 26-like intrinsic protein family of plant aquaglyceroporins. *Biochim. Biophys. Acta* **1758**, 1165–1175 https://doi.org/10.1016/j.bbamem.2006.03.024
50 Di Giorgio, J.A., Bienert, G.P., Ayub, N.D., Yaneff, A., Barberini, M.L., Mecchia, M.A. et al. (2016) Pollen-Specific aquaporins NIP4;1 and NIP4;2 are required for pollen development and pollination in *Arabidopsis thaliana*. *Plant Cell* **28**, 1053–1077 https://doi.org/10.1105/tpc.15.00776
51 Wang, S., Yoshinari, A., Shimada, T., Hara-Nishimura, I., Mitani-Ueno, N., Ma, J.F. et al. (2017) Polar localization of the NIP5;1 boric acid channel is maintained by endocytosis and facilitates boron transport in Arabidopsis roots. *Plant Cell* **29**, 824–842 https://doi.org/10.1105/tpc.16.00825
52 Klipp, R.C., Cullinan, M.M. and Bankston, J.R. (2020) Insights into the molecular mechanisms underlying the inhibition of acid-sensing ion channel 3 gating by stomatin. *J. Gen. Physiol.* **152**, e201912471 https://doi.org/10.1085/jgp.201912471
53 Bellati, J., Champeyroux, C., Hem, S., Rofidal, V., Krouk, G., Maurel, C. et al. (2016) Novel aquaporin regulatory mechanisms revealed by interactomics. *Mol. Cell. Proteomics* **15**, 3473–3487 https://doi.org/10.1074/mcp.M116.060087
54 Prado, K., Cotelle, V., Li, G., Bellati, J., Tang, N., Tournaire-Roux, C. et al. (2019) Oscillating aquaporin phosphorylation and 14-3-3 proteins mediate the circadian regulation of leaf hydraulics. *Plant Cell* **31**, 417–429 https://doi.org/10.1105/tpc.18.00804

55 Saier, M.H., Reddy, V.S., Tamang, D.G. and Västermark, A. (2014) The transporter classification database. *Nucleic Acids Res.* **42**, D251–D258 https://doi.org/10.1093/nar/gkt1097
56 Lu, F., Li, S., Jiang, Y., Jiang, J., Fan, H., Lu, G. et al. (2011) Structure and mechanism of the uracil transporter UraA. *Nature* **472**, 243–245 https://doi.org/10.1038/nature09885
57 Arakawa, T., Kobayashi-Yurugi, T., Alguel, Y., Iwanari, H., Hatae, H., Iwata, M. et al. (2015) Crystal structure of the anion exchanger domain of human erythrocyte band 3. *Science* **350**, 80–84 https://doi.org/10.1126/science.aaa4335
58 Thurtle-Schmidt, B.H. and Stroud, R.M. (2016) Structure of Bor1 supports an elevator transport mechanism for SLC4 anion exchangers. *Proc. Natl. Acad. Sci. U.S.A.* **113**, 10542–10546 https://doi.org/10.1073/pnas.1612603113
59 Geertsma, E.R., Chang, Y.N., Shaik, F.R., Neldner, Y., Pardon, E., Steyaert, J. et al. (2015) Structure of a prokaryotic fumarate transporter reveals the architecture of the SLC26 family. *Nat. Struct. Mol. Biol.* **22**, 803–808 https://doi.org/10.1038/nsmb.3091
60 Alguel, Y., Amillis, S., Leung, J., Lambrinidis, G., Capaldi, S., Scull, N.J. et al. (2016) Structure of eukaryotic purine/H+ symporter UapA suggests a role for homodimerization in transport activity. *Nat. Commun.* **7**, 1–9 https://doi.org/10.1038/ncomms11336
61 Huynh, K.W., Jiang, J., Abuladze, N., Tsirulnikov, K., Kao, L., Shao, X. et al. (2018) CryoEM structure of the human SLC4A4 sodium-coupled acid-base transporter NBCe1. *Nat. Commun.* **9**, 900 https://doi.org/10.1038/s41467-018-03271-3
62 Garaeva, A.A and Slotboom, D.J (2020) Elevator-type mechanisms of membrane transport. *Biochem. Soc. Trans.* **48**, 1227–1241 https://doi.org/10.1042/BST20200290
63 Burtscher, V., Schicker, K., Freissmuth, M. and Sandtner, W. (2019) Kinetic models of secondary active transporters. *Int. J. Mol. Sci.* **20**, 5365 https://doi.org/10.3390/ijms20215365
64 Macara, I.G. and Cantley, L.C. (1981) Interactions between transport inhibitors at the anion binding sites of the Band 3 dimer. *Biochemistry* **29**, 5095–5105 https://doi.org/10.1021/bi00521a001
65 Yermiyahu, U., Ben-Gal, A., Keren, R. and Reid, R.J. (2008) Combined effect of salinity and excess boron on plant growth and yield. *Plant Soil* **304**, 73–87 https://doi.org/10.1007/s11104-007-9522-z
66 Corradi, V., Mendez-Villuendas, E., Ingólfsson, H.I., Gu, R.-X., Siuda, I., Melo, M.N., et al. (2018) Lipid–protein interactions are unique fingerprints for membrane proteins. *ACS Cent. Sci.* **4**, 709–717 https://doi.org/10.1021/acscentsci.8b00143
67 Kalli, A.C. and Reithmeier, R.A. (2018) Interaction of the human erythrocyte Band 3 anion exchanger 1 (AE1, SLC4A1) with lipids and glycophorin A: Molecular organization of the Wright (Wr) blood group antigen. *PLOS Comput. Biol.* **14**, e1006284 https://doi.org/10.1371/journal.pcbi.1006284
68 Parker, J.L. and Newstead, S. (2014) Molecular basis of nitrate uptake by the plant nitrate transporter NRT1.1. *Nature* **507**, 68–72 https://doi.org/10.1038/nature13116
69 Sun, J., Bankston, J.R., Payandeh, J., Hinds, T.R., Zagotta, W.N. and Zheng, N. (2014) Crystal structure of the plant dual-affinity nitrate transporter NRT1.1. *Nature* **507**, 73–77 https://doi.org/10.1038/nature13074
70 Rashid, M., Bera, S., Banerjee, M., Medvinsky, A.B., Sun, G.-Q., Li, B.-L. et al. (2020) Feedforward control of plant nitrate transporter NRT1.1 biphasic adaptive activity. *Biophys. J.* **118**, 898–908 https://doi.org/10.1016/j.bpj.2019.10.018
71 Claassens, N.J., Burgener, S., Vögeli, B., Erb, T.J. and Bar-Even, A. (2019) A critical comparison of cellular and cell-free bioproduction systems. *Curr. Opin. Biotechnol.* **60**, 221–229 https://doi.org/10.1016/j.copbio.2019.05.003
72 Shadiac, N., Nagarajan, Y., Waters, S. and Hrmova, M. (2013) The close allies in membrane protein research: cell-free synthesis and nanotechnology. *Mol. Membr. Biol.* **30**, 229–245 https://doi.org/10.3109/09687688.2012.762125
73 Periasamy, A., Shadiac, N., Amalraj, A., Garajová, S., Nagarajan, Y., Waters, S. et al. (2013) Cell-free protein synthesis of membrane (1,3)-β-d-glucan (curdlan) synthase: co-translational insertion in liposomes and reconstitution in nanodiscs. *Biochim. Biophys. Acta Biomembr.* **1828**, 743–757 https://doi.org/10.1016/j.bbamem.2012.10.003
74 Ayoubi-Joshaghan, M.A., Dianat-Moghadam, H., Seidi, K., Jahanban-Esfahalan, A., Zare, P. and Jahanban-Esfahlan, R. (2020) Cell-free protein synthesis: The transition from batch reactions to minimal cells and microfluidic devices. *Biotech. Bioeng.* **117**, 1204–1229 https://doi.org/10.1002/bit.27248
75 Feroz, H., Meisenhelter, J., Jokhadze, G., Bruening, M. and Kumar, M. (2019) Rapid screening and scale-up of ultracentrifugation-free, membrane-based procedures for purification of His-tagged membrane proteins. *Biotechnol. Prog.* **35**, e2859 https://doi.org/10.1002/btpr.2859
76 Guo, Y. (2020) Be cautious with crystal structures of membrane proteins or complexes prepared in detergents crystals. *Crystals* **10**, 86 https://doi.org/10.3390/cryst10020086
77 Knowles,, T.J., Finka, R., Smith, C., Lin, Y.-P., Dafforn, T. and Overduin, M. (2009) Membrane proteins solubilized intact in lipid containing nanoparticles bounded by styrene maleic acid copolymer. *J. Am. Chem. Soc.* **131**, 7484–7485 https://doi.org/10.1021/ja810046q
78 Burridge, K.M., Harding, B.D., Sahu, I.D., Kearns, M.M., Stowe, R.B., Dolan, M.T. et al. (2020) Simple derivatization of RAFT-synthesized styrene-maleic anhydride copolymers for lipid disk formulations. *Biomacromolecules* **21**, 1274–1284 https://doi.org/10.1021/acs.biomac.0c00041
79 Parmar, M., Rawson, S., Scar, C.A., Goldman, A., Daorn, T.R., Muench, S.P. et al. (2018) Using a SMALP platform to determine a sub-nm single particle cryo-EM membrane protein structure. *Biochim. Biophys. Acta Biomembr.* **1860**, 378–383 https://doi.org/10.1016/j.bbamem.2017.10.005
80 Nannenga, B.L. and Gonen, T. (2019) The cryo-EM method microcrystal electron diffraction (MicroED). *Nat. Methods* **16**, 369–379 https://doi.org/10.1038/s41592-019-0395-x
81 Chen, R., Huang, C.-Y., Hennig, M., Nar, H. and Schnapp, G. (2020) *In situ* crystallography as an emerging method for structure solution of membrane proteins: the case of CCR2A. *FEBS J.* **287**, 866–873 https://doi.org/10.1111/febs.15098
82 Beale, J.H. (2020) Macromolecular X-ray crystallography: soon to be a road less travelled? *Acta Crystallogr. D Struct Biol.* **76**, 400–405 https://doi.org/10.1107/S2059798320004660
83 Coates, L. (2020) Ion permeation in potassium ion channels. *Acta Crystallogr. D Struct Biol.* **76**, 326–331 https://doi.org/10.1107/S2059798320003599
84 Yamamoto, T., Hoshikawa, K., Ezura, K., Okazawa, R., Fujita, S., Takaoka, M. et al. (2018) Improvement of the transient expression system for production of recombinant proteins in plants. *Sci. Rep.* **8**, 4755 https://doi.org/10.1038/s41598-018-23024-y
85 Schillberg, S., Raven, N., Spiegel, H., Rasche, S. and Buntru, M. (2019) Critical analysis of the commercial potential of plants for the production of recombinant proteins. *Front. Plant Sci.* **10**, 720 https://doi.org/10.3389/fpls.2019.00720

Biochemical Society Transactions (2020) **48** 1683–1696
https://doi.org/10.1042/BST20200164

86 Abd-Aziz, N., Tan, B.C., Rejab, N.A., Othman, R.Y. and Khalid, N. (2020) A new plant expression system for producing pharmaceutical proteins. *Mol. Biotechnol.* **62**, 240–251 https://doi.org/10.1007/s12033-020-00242-2

87 Routledge, S.J., Linney, J.A. and Goddard, A.D. (2019) Liposomes as models for membrane integrity. *Biochem. Soc. Trans.* **47**, 919–932 https://doi.org/10.1042/BST20190123

88 Petukhov, M.V., Konarev, P.V., Dadinova, L.A., Fedorova, N.V., Volynsky, P.E., Svergun, D.I. et al. (2020) Quasi-atomistic approach to modeling of liposomes. *Cryst. Rep.* **65**, 258–263 https://doi.org/10.1134/S1063774520020182

89 Tietz, S., Leuenberger, M., Höhner, R., Olson, A.H., Fleming, G.R. and Kirchhoff, H. (2020) A proteoliposome-based system reveals how lipids control photosynthetic light harvesting. *J. Biol. Chem.* **295**, 1857–1866 https://doi.org/10.1074/jbc.RA119.011707

90 Martinière,, S., Gibrat,, R., Sentenac,, H., Dumont,, X., Gaillard,, I. and Paris,, N. (2018) Uncovering pH at both sides of the root plasma membrane interface using noninvasive imaging. *Proc. Natl. Acad. Sci. U.S.A.* **115**, 6488–6493 https://doi.org/10.1073/pnas.1721769115

91 Smart, O.S., Neduvelil, J.G., Wang, X., Wallace, B.A. and Sansom, M.S.P. (1996) HOLE: a program for the analysis of the pore dimensions of ion channel structural models. *J. Mol. Graph.* **14**, 354–360 https://doi.org/10.1016/S0263-7855(97)00009-X